A STUDY OF BROADBAND HOT-CARRIER DIODE MIXERS

By

Ersin Güler

United States
Naval Postgraduate School

THESIS

A STUDY OF BROADBAND
HOT-CARRIER DIODE MIXERS

by

Ersin Güler

December 1970

A Study of Broadband

Hot-Carrier Diode Mixers

by

Ersin Güler
Lieutenant (junior grade), Turkish Navy
B.S., Naval Postgraduate School, 1970

Submitted in partial fulfillment of the
requirements for the degree of

MASTER OF SCIENCE IN ELECTRICAL ENGINEERING

from the

NAVAL POSTGRADUATE SCHOOL
December 1970

ABSTRACT

A theory is derived for single diode, single-balanced, and double-balanced mixers. An interfering signal is assumed to be present in order to analyze intermodulation and cross-modulation distortions.

Measurements are made in the 50 - 200 MHz range and close agreement with the theory is found for conversion loss. Disagreement in RF and LO isolations is attributed to stray capacitances. It is also shown that circuit-board and transformer design greatly affects performance of a mixer.

A comparison of the single diode, single-balanced, and double-balanced mixers is given and it is indicated that the double-balanced mixer is superior.

TABLE OF CONTENTS

LIST OF TABLES

LIST OF DRAWINGS

ACKNOWLEDGEMENT

The author wishes to express his appreciation to Professor R. W. Adler for the invaluable aid and counsel which he has offered during the preparation of this thesis.

I. INTRODUCTION

A mixer is a network containing one or more nonlinear devices which combines two unrelated signals to obtain a third signal, at the sum or difference frequency. Mixers are extensively utilized in communication receivers and transmitters, radars, and control systems.

Frequencies other than the sum and difference frequency are generated by the mixing action, and they are called spurious responses. It will be shown that spurious responses generated by input (RF) and local oscillator (LO) signals are:

$$f_{IF} = nf_1 \pm mf_p$$

where

f_1 is the signal frequency (RF),

f_p is the LO frequency,

f_{IF} is the intermediate frequency (IF),

m,n are harmonic numbers of RF and LO frequencies.

The desired output of the mixer occurs when m=n=1. Spurious responses occur at the frequencies for which m or $n \neq 1$. The spurious responses can be reduced in number by means of selective circuits (filters) at the mixer output.

A large signal, f_2, close to signal frequency can interact with the signal to produce third-order intermodulation (IM) distortion at frequencies $2f_2 \pm f_1$ and $2f_1 \pm f_2$.

If f_1 and f_2 are arbitrarily close to one another the third-order IM signals are close to the input signal, f_1, and will generate frequencies within the filter bandwidth at the mixer output. The change in the amplitude of the interfering signal, f_2, will also cross-modulate the output.

Spurious responses and IM distortions can be reduced or completely eliminated by careful mixer design. Therefore mixer design becomes extremely important in high level signal environments in establishing receiver performance. There is a need to design mixers with the widest possible dynamic range and low conversion loss.

Nonlinear devices typically employed by mixers are vacuum tubes, semiconductor diodes, bipolar transitors and FET's. In this study attention will be focused on passive broadband mixers using hot-carrier diodes.

A hot-carrier diode junction consists of a metal and a semiconductor rather than two semiconductors with an energy barrier, known as Schotty barrier, which occurs because of the difference in the work functions of the two materials. The barrier is decreased by forward bias and increased by reverse bias, hence the barrier results in a rectifying diode. In the forward bias condition the majority carriers (electrons) are injected from the semiconductor to the metal in a very short time. The flow of electrons occurs with virtually no flow of minority carriers in the reverse direction. Consequently, the response to a change is much faster than in p-n junctions. Therefore, hot-carrier diodes have higher frequency capabilities as

compared to p-n junction and point contact diodes. Their improved electrical performance, low noise, and nearly ideal characteristics result in high conversion efficiency making hot-carrier diodes superior to other nonlinear devices, especially in high frequency mixer applications.

The single diode mixer, Figure 1a, has poor port-to-port isolation and does not offer any means of eliminating spurious responses and IM distortions. Conversion loss (L_c) is higher compared to other configurations.

The single-balanced mixer, Figure 1b, has better isolation and conversion loss and removes the spurious responses generated by the even harmonics of the input signal.

The double-balanced mixer, Figure 1c, has even better isolation compared to the single-balanced mixer. A double-balanced mixer allows energy to be exchanged on a full-wave cycle rather than half cycle, therefore, offers higher efficiency and lower conversion loss. Spurious responses generated by the even harmonics of the signal and LO frequencies are eliminated. Thus the output ideally does not contain any third-order spurious responses, which are one of the most troublesome distortion terms in mixers.

Layout becomes extremely important for both balanced configurations especially at high frequencies. Nearly perfect balance can be obtained by symmetrical layout and using careful VHF construction techniques: short leads and short ground returns. Wide bandwidth is obtained by designing toroidal transformers with tight coupling between the windings and carefully choosing the core material.

Theoretical analysis is given in Section II for the mixers in Figure 1. The circuits are designed and tested within the 50 to 200 MHz range in order to verify the theoretical results. In the experiment two different core materials are used to demonstrate the importance of the choice. Low cost commercially available cores were used, therefore the bandwidth was limited. IM products are not measured because the spectrum analyzer used generates so many spurious responses within itself, it is virtually impossible to observe those of the circuits under test. Cross-modulation (CM) distortion is also not demonstrated because the low level output of the signal generators did not produce CM terms of sufficient amplitude for oscilloscope viewing. A comparison of the theory and experiment is given and advantages and disadvantages of the configurations and construction details are specified in Section III.

II. THEORETICAL ANALYSIS

In the following discussion the performance of the single diode mixer, single-balanced mixer, and double-balanced mixer is given. In order to compare the behavior of the different configurations with respect to spurious responses, IM and CM distortions, an interfering signal is assumed to be present. For this comparison, a good understanding of the spurious response, IM and CM distortion is necessary. Therefore, the following definitions are given:

Spurious responses occur at $nf_1 \pm mf_p$ for n or $m \neq 1$ and can be reduced by biasing or mixer design. Therefore, a bias voltage, V_b, is included in the analysis.

IM responses are formed when the mixer is subjected to one or more undesired signals. Two or more signals and the LO signal can mix and produce IM responses at frequencies which are represented by any linear combination of the input frequencies:

$$f_{IF} = nf_1 \pm kf_2 \pm qf_2 \pm mf_p \qquad \text{(II-1)}$$

Equation (II-1) accounts for IM responses in the mixer stage. Two undesired signals can mix and generate the desired signal due to the nonlinearities in the previous stages. This is also called IM response and named receiver intermodulation.

Cross-modulation response occurs when the modulation on an undesired signal is transferred to a desired signal.

CM is only modulation transfer rather than the frequency translation.

IM and CM distortions cannot be eliminated by mixer design but IM responses can be reduced. Ideal transformers are assumed in this analysis.

A. SINGLE DIODE MIXER

The current flowing through the diode in Figure 1a is:

$$i_1 = I_s(e^{\frac{q}{nkT}v} - 1) \qquad \text{(II-2)}$$

where,

I_s = Reverse saturation current of the diode,

v = voltage across the diode,

q = electron charge = $1.6\text{x}10^{-19}$ coulombs,

n = diode ideality factor = 1.05 for the diodes used,

k = Boltzmann's constant = $1.38\text{x}10^{-23}$ Joules/°K,

and T = temperature in °K.

To simplify the deviations α is defined to be,

$$\alpha \equiv \frac{q}{nkT} .$$

The voltage across the diode is:

$$v = V_b + V_1\cos\omega_1 t + V_2\cos\omega_2 t + V_p\cos\omega_p t$$

where,

V_b is the DC bias voltage,

V_1 and ω_1 are the amplitude and frequency of the input signal,

V_p and ω_p are the amplitude and frequency of the LO signal,

V_2 and ω_2 are the amplitude and frequency of the interfering signal.

Since transformers are assumed to be ideal, reflected impedances and transformer losses are not present. Therefore,

$$i_L = i_1$$

or

$$i_L = I_s \left[e^{\alpha(V_b+V_1\cos\omega_1 t+V_2\cos\omega_2 t+V_p\cos\omega_p t)} - 1 \right]$$

Using the identity,

$$e^{\cos\theta} = I_o(x)+2\sum_{r=1}^{\infty} I_r(x)\cos r\theta \qquad \text{(II-3)}$$

where,

$I_o(x)$ and $I_r(x)$ are the Modified Bessel functions of the first kind.

i_L is found as follows:

$$i_L = I_s \Big\{ e^{\alpha V_b} \Big[I_o(\alpha V_1) I_o(\alpha V_2) I_o(\alpha V_p)$$

$$+2I_o(\alpha V_2) I_o(\alpha V_p) \sum_{n=1}^{\infty} I_n(\alpha V_1)\cos n\omega_1 t$$

$$+2I_o(\alpha V_1) I_o(\alpha V_p) \sum_{k=1}^{\infty} I_k(\alpha V_2)\cos k\omega_2 t$$

$$+2I_o(\alpha V_1) I_o(\alpha V_2) \sum_{m=1}^{\infty} I_m(\alpha V_p)\cos m\omega_p t$$

$$+2I_o(\alpha V_p) \sum_{n=1}^{\infty} \sum_{k=1}^{\infty} I_n(\alpha V_1) I_k(\alpha V_2)\cos(k\omega_2 \pm n\omega_1)t$$

$$+2I_o(\alpha V_2)\sum_{n=1}^{\infty} \sum_{m=1}^{\infty} I_n(\alpha V_1)I_m(\alpha V_p)\cos(n\omega_1 \pm m\omega_p)t$$

$$+2I_o(\alpha V_1)\sum_{k=1}^{\infty} \sum_{m=1}^{\infty} I_k(\alpha V_2)I_m(\alpha V_p)\cos(k\omega_2 \pm m\omega_p)t$$

$$+2\sum_{n=1}^{\infty} \sum_{k=1}^{\infty} \sum_{m=1}^{\infty} I_n(\alpha V_1)I_k(\alpha V_2)I_m(\alpha V_p)$$

$$\cos(n\omega_1 \pm k\omega_2 \pm m\omega_p)t \Big] - 1 \Big\}. \qquad \text{(II-4)}$$

The complete derivation is given in Appendix A.

The output voltage is

$$v_{IF} = R_L i_L .$$

Output at the IF frequency becomes

$$v_{IF} = 2R_L I_s e^{\alpha V_b} I_o(\alpha V_2)I_1(\alpha V_1)I_1(\alpha V_p)\cos(\omega_1 \pm \omega_p)t.$$

If the interfering signal is not present, then

$$I_o(o)=1.0$$

and

$$v_{IF} = 2R_L I_s e^{\alpha V_b} I_1(\alpha V_1)I_1(\alpha V_p)\cos(\omega_1 \pm \omega_2)t.$$

Since the output amplitude is modulated with the interfering signal amplitude, $I_o(\alpha V_2)$ represents the CM distortion term at the IF frequency.

All spurious responses are present at the output. The term

$$2e^{\alpha V_b} R_L I_s \sum_{n=1}^{\infty} \sum_{k=1}^{\infty} \sum_{m=1}^{\infty} I_n(\alpha V_1)I_k(\alpha V_2)I_m(\alpha V_p)$$

$$\cos(n\omega_1 \pm k\omega_2 \pm m\omega_p)t$$

gives the IM products.

The most troublesome IM distortion is the third-order IM product, which is

$$2R_L I_s e^{\alpha V_b} I_1(\alpha V_1) I_2(\alpha V_2) I_1(\alpha V_p) \cos(-\omega_1 + 2\omega_2 \pm \omega_p)t$$

or

$$2R_L I_s e^{\alpha V_b} I_2(\alpha V_1) I_1(\alpha V_2) I_1(\alpha V_p) \cos(2\omega_1 - \omega_2 \pm \omega_p)t.$$

If ω_2 is close to ω_1 third-order IM distortions will always be present at the output even if a filter is used.

RF and LO input signal isolation levels can be calculated by:

$$2I_s R_L e^{\alpha V_b} I_1(\alpha V_1) I_o(\alpha V_2) I_o(\alpha V_p) \cos\omega_1 t$$

and

$$2I_s R_L e^{\alpha V_b} I_o(\alpha V_1) I_o(\alpha V_2) I_1(\alpha V_p) \cos\omega_p t.$$

B. SINGLE-BALANCED MIXER

Figure 2a is an equivalent circuit for Figure 1b. Currents through the diodes D_1 and D_2 are, respectively,

$$i_1 = I_{s_1} (e^{\alpha_1 v_1} - 1) \qquad \text{(II-5)}$$

$$i_2 = I_{s_2} (e^{\alpha_2 v_2} - 1) \qquad \text{(II-6)}$$

Perfect balance can be obtained by using identical diodes. Therefore,

$$I_{s_1} = I_{s_2} = I_s$$

$$\alpha_1 = \alpha_2 = \alpha$$

and

$$V_{b_1} = V_{b_2} = V_b$$

Voltages across the diodes are:

$$v_1 = V_b + V_1\cos\omega_1 t + V_2\cos\omega_2 t + V_p\cos\omega_p t \qquad \text{(II-7)}$$

and

$$v_2 = V_b - V_1\cos\omega_1 t - V_2\cos\omega_2 t + V_p\cos\omega_p t \; . \qquad \text{(II-8)}$$

Current through the load resistance is

$$i_L = i_1 - i_2 \; . \qquad \text{(II-9)}$$

Then, substituting equations (II-7) and (II-8) into equations (II-5) and (II-6), respectively, the result into equation (II-9) the following expression for i_L is obtained

$$\begin{aligned} i_L = I_s\, e^{\alpha V_b}\Bigg[& 4I_o(\alpha V_2)I_o(\alpha V_p) \sum_{n=1,3,5,\ldots}^{\infty} I_n(\alpha V_1)\cos n\omega_1 t \\ & + 4I_o(\alpha V_1)I_o(\alpha V_p) \sum_{k=1,3,5,\ldots}^{\infty} I_k(\alpha V_2)\cos k\omega_2 t \\ & + 4I_o(\alpha V_p) \sum_{n=1,3,5,\ldots}^{\infty} \sum_{k=1,3,5,\ldots}^{\infty} I_n(\alpha V_1)I_k(\alpha V_2)\cdot \\ & \cos(n\omega_1 \pm k\omega_2)t \\ & + 4I_o(\alpha V_1) \sum_{k=1,3,5,\ldots}^{\infty} \sum_{m=1}^{\infty} I_k(\alpha V_2)I_m(\alpha V_p)\cos(k\omega_2 \pm m\omega_p)t \\ & + 4I_o(\alpha V_2) \sum_{n=1,3,5,}^{\infty} \sum_{m=1}^{\infty} I_n(\alpha V_1)I_m(\alpha V_p)\cos(n\omega_1 \pm m\omega_p)t \\ & + 4 \sum_{\substack{n=1,3,5,\ldots \\ n=2,4,6,}}^{\infty} \sum_{\substack{k=2,4,6,\ldots \\ k=1,3,5,}}^{\infty} \sum_{m=1}^{\infty} I_n(\alpha V_1)I_k(\alpha V_2)I_m(\alpha V_p)\cdot \\ & \cos(n\omega_1 \pm k\omega_2 \pm m\omega_p)t \Bigg] \; . \end{aligned} \qquad \text{(II-10)}$$

Complete analysis is given in Appendix B. It is seen from equation (II-10), that in the single-balanced mixer spurious responses due to even harmonics of the input signal are eliminated. Perfect LO signal isolation is obtained and even harmonics of the RF signal are removed. Third-order

IM distortion is reduced, since it appears only due to the odd harmonics of the input signal and even harmonics of the interference signal, or vice versa, but not both.

The IF output voltage

$$v_{IF} = 4I_s R_L e^{\alpha V_b} I_o(\alpha V_2) I_1(\alpha V_1) I_1(\alpha V_p) \cos(\omega_1 \pm \omega_p)t$$

is twice that of the single diode mixer. Thus, conversion loss is improved by 6dB compared to the single diode mixer.

C. DOUBLE-BALANCED MIXER

The equivalent circuit for the double-balanced mixer is shown in Figure 2b. The diodes are assumed to be matched, therefore, their parameters are identical and DC bias voltages are not needed.

Currents through the diodes are

$$i_1 = I_s(e^{\alpha v_1} - 1),$$

$$i_2 = I_s(e^{\alpha v_2} - 1),$$

$$i_3 = I_s(e^{\alpha v_3} - 1),$$

and

$$i_4 = I_s(e^{\alpha v_4} - 1)$$

where

$$v_1 = V_1 \cos\omega_1 t + V_2 \cos\omega_2 t + V_p \cos\omega_p t$$

$$v_2 = -V_1 \cos\omega_1 t - V_2 \cos\omega_2 t + V_p \cos\omega_p t$$

$$v_3 = -V_1 \cos\omega_1 t - V_2 \cos\omega_2 t - V_p \cos\omega_p t$$

$$v_4 = V_1 \cos\omega_1 t + V_2 \cos\omega_2 t - V_p \cos\omega_p t$$

and $i_L = i_1 - i_2 + i_3 - i_4$.

Using the above equations the load current can be derived. The result is

$$\frac{i_L}{I_s} = 8I_o(\alpha V_2) \sum_{n=1,3,5,\cdots}^{\infty} \sum_{m=1,3,5,\cdots}^{\infty} I_n(\alpha V_1) I_m(\alpha V_p) \cdot \cos(n\omega_1 \pm m\omega_p)t$$

$$+8I_o(\alpha V_1) \sum_{k=1,3,5,\cdots}^{\infty} \sum_{m=1,3,5,\cdots}^{\infty} I_k(\alpha V_2) I_m(\alpha V_p) \cdot \cos(k\omega_2 \pm m\omega_p)t$$

$$+8 \sum_{\substack{n=1,3,5,\cdots \\ n=2,4,6,\cdots}}^{\infty} \sum_{\substack{k=2,4,6,\cdots \\ k=1,3,5,\cdots}}^{\infty} \sum_{m=1,3,5,\cdots}^{\infty} I_n(\alpha V_1) I_k(\alpha V_2) I_m(\alpha V_p) \cos(n\omega_1 \pm k\omega_2 \pm m\omega_p)t \quad .$$

Complete details are contained in Appendix C.

In the double-balanced mixer spurious responses due to the even harmonics of both RF and LO signals are eliminated. Perfect RF and LO signal isolation is obtained, and IM products are reduced, compared to the single-balanced and single diode mixers.

The IF output voltage is twice that of the single-balanced mixer. Therefore, conversion loss is improved 6dB with respect to the single-balanced mixer and 12dB compared to the single diode mixer.

III. EXPERIMENTAL RESULTS

Experimental work was performed to verify the theoretical analysis and to make a comparison of the mixer types in Figure 1. The main consideration in the choice of the elements was to obtain minimum conversion loss with high port-to-port isolation for the widest possible dynamic range and bandwidth.

A. CIRCUIT-BOARD DESIGN

Several different layouts were designed for the single-balanced and especially for the double-balanced mixers, with Figure 3 representing the finalized forms in one-to-one scale. The circuit-board design depends upon which ports of the mixer circuit are used as RF, LO, and IF. An initial layout for the double-balanced mixer was similar to Figure 1c, but with RF, LO, IF connected to 9, 1, 7 respectively, and 4 grounded. Although this allowed for a more symmetrical layout and 7dB conversion loss, the RF isolation was a very poor 8dB. The circuit of Figure 1c yielded 36dB RF isolation with 9dB conversion loss. The difference of 28dB RF isolation is due to unbalance in the output transformer. This study proved that the better the symmetry in circuit-board, the lower the conversion loss. The ground stripes crossing through the board, used in the single-balanced mixer layout, reduce stray capacitances and result in a small change in conversion loss as the frequency is increased. The double-balanced mixer cannot take advantage

of these ground stripes and still benefit by short diode lead lengths and suffers a greater change in conversion loss with frequency.

B. TRANSFORMERS

The transformers are wound on Micro-Metals, Type T 37-13 (50-120 MHz) and T 37 (100-200 MHz) powdered iron toroids. The influence of the core material on mixer performance will be discussed later in this section. Coupling between the wires directly affects the bandwidth of the mixer. Thus, the windings must be as tight as possible. This is accomplished by twisting the three wires together and tightly winding them on the toroid. Twelve trifilar turns of number 27 enameled wire are wound on each toroid, except for the transformer at the output of the single diode mixer. The following diagram identifies the primary, secondary, and center-tap leads:

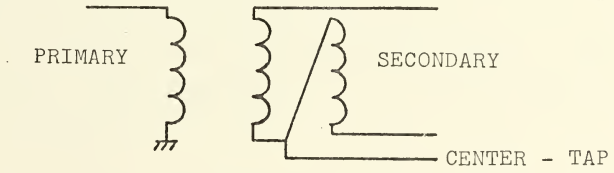

A one-to-one transformer ratio is selected because of ease in construction. Ratios other than one-to-one will affect the operating point of the diodes due to reflected impedances (Reference 7) and will change the current through the diode. But it is shown in the theoretical analysis the output current is the difference of diode currents

for both balanced mixers, therefore, a transformation ratio other than one-to-one will result in only complicating the transformer design in terms of balance. Toroid choice becomes important in terms of conversion loss. This can be tested by replacing the T 37-13 toroids with T 37-0's and by observing the change in conversion loss. In the experiment this was conducted for the single-balanced mixer and a 5dB increase in conversion loss was measured. Then by removing the output transformer, which requires inverting one of the diodes to obtain balance, about 2.5dB improvement in conversion loss was observed. Thus the quality of the toroid is a major factor in conversion loss, since this 5dB of change is appreciable.

C. HOT-CARRIER DIODES

Hewlett-Packard 5082-2815 (matched quad) hot-carrier diodes are used in the double-balanced mixer as well as in the single diode and single-balanced mixers, so that the effect of differences in diode parameters on mixer performance is minimized. The advantages of hot-carrier diodes were given in Section I.

D. EXPERIMENT AND LIMITATIONS

An experiment was conducted in 50 to 200 MHz range using the set-up in Figure 4 with the equipment indicated on the diagram. The reference generator was set to the 30 MHz IF frequency and used to measure the output power of the mixer by the comparison method. Since the difference

in RF and IF outputs gives the conversion loss, this information was also obtained. Isolation was measured in the same manner.

Limiting effects for the 150 MHz bandwidth are the layout and the toroids used. Table I shows that there is a 1.1 and 1.6dB difference in conversion loss between the theoretical and measured values for the single-balanced and double-balanced mixers. This difference varies irregularly in RF and LO isolation for all mixer types. These differences are caused by stray capacitances (circuit-board design effect) and by transformer losses (toroid effect). At frequencies out of the 50-200 MHz range losses increase rapidly.

The dynamic range of a mixer is a function of LO power and IM and spurious responses. Due to the limited output of the signal generators, the upper limit of the dynamic range was restricted to -10dbm. The lower limit was -50dbm, set by the noise figure of the spectrum analyzer.

E. RESULTS AND COMPARISON

Measured 30 MHz IF output versus RF power plots are shown in Figure 5, 6, and 7 for the single diode, single-balanced and double-balanced mixers with 5, 0, and 0 dbm LO power respectively. Theoretical values are not shown on the figures but instead are given in Table 1 in order to compare the mixers that are tested.

The difference in conversion loss between the theory and experiment for both balanced mixers was explained in

Section IID. For the single diode mixer this difference is 5.5dB greater and is due to impedances reflected through the transformers to the diode loop. These impedances will decrease the diode current, thus the output voltage and increase the conversion loss. Although the same effect is present for each diode in both balanced mixers, the load current is the difference of the diode currents, thus is cancelled at the IF output.

As indicated in Table I, theoretical RF and LO isolations do not agree with the experiment. The difference of 16dB RF isolation for both the single diode and single-balanced mixers is attributed to the reflected impedance and transformer losses. The same argument is valid for the single diode mixer LO isolation disagreement. For the single and double-balanced mixers perfect isolation is not achieved due to the coupling effect of stray capacitances between the input and output ports.

In the theoretical analysis it is shown that the output current is proportional to the LO voltage. Therefore, conversion loss depends upon the LO drive level - the higher the LO voltage the lower the conversion loss (below the point where compression begins). This is demonstrated in Figure 8 by the measured values of conversion loss versus LO power for the double-balanced mixer.

The double-balanced mixer is superior to the single-balanced and single diode mixers in conversion loss, RF and LO isolation. Lower conversion loss also results in a

wider dynamic range. Theory shows spurious responses due to the even harmonics of both RF and LO signals are eliminated and IM responses due to the even harmonics of the LO signal are also eliminated in the double-balanced mixer, although the third-order IM response is the same as in the single-balanced mixer.

IV. CONCLUSION

As mentioned in the Introduction, mixer design becomes extremely important in high level signal environment in establishing receiver performance. Therefore, there is a need to design mixers with the widest possible dynamic range, low conversion loss, and minimum IM distortion and other spurious responses.

In this study the theory for the single diode and single and double-balanced mixers was given in the presence of an interfering signal and it was shown that CM distortion cannot be eliminated at the mixer stage, but for balanced mixers, IM and spurious responses can be reduced. It was also indicated that the conversion loss in the double-balanced mixer is improved 6dB compared to the single-balanced mixer and 12dB with respect to the single diode mixer. RF and LO isolations were found to be perfect for the double-balanced mixer, while for the single-balanced mixer they were 10dB and perfect, and for a single diode mixer were both 4dB.

Close agreement with the theory and experiment was found for conversion loss in both balanced mixer configurations with the 6dB discrepancy in the single diode mixer case being explained by the reflected impedances. In all cases, RF and LO isolation disagreement with the theory and the experiment was found to be greater. The most likely explanation indicated stray capacitances, transformer losses,

and unbalance in the circuits. An increase in frequency decreased both RF and LO isolations and indicated that effect of stray capacitances.

Experiment also showed that the symmetry of the circuit-board and choice of the core material affects the performance in terms of conversion loss and isolations.

Through both theory and experimental work it has been shown that the double-balanced mixer enjoys a better conversion loss which implies wider dynamic range together with RF and LO isolation and a minimum number of spurious and IM responses, compared to the single diode and single-balanced mixer.

Further study should be undertaken to examine IM distortion in double-balanced mixers. Theoretical analysis shows that the third-order IM terms are the maximum amplitude IM products and restrict the dynamic range of the mixer. Measurements should be conducted and design improvement techniques investigated in terms of IM product reduction.

Since the measuring equipment used in this study severely limited the experimental evaluations, meaningful measurements can only be made by using a spectrum analyzer and signal generator which are not currently available commercially. The requirement on the analyzer of very low internally-generated spurious responses might be met by replacing its mixer with a hot-carrier diode double-balanced mixer. A "clean", relatively high-output signal

generator would probably necessitate the development of a suitable Class A post-amplifier to boost the output of standard generators.

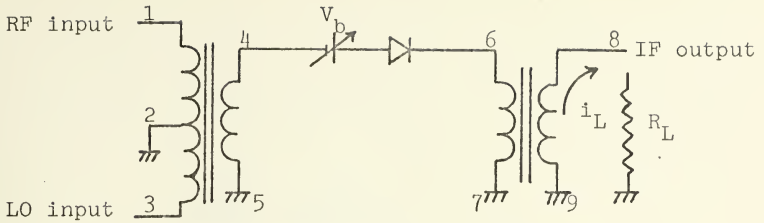

a. Single Diode Mixer.

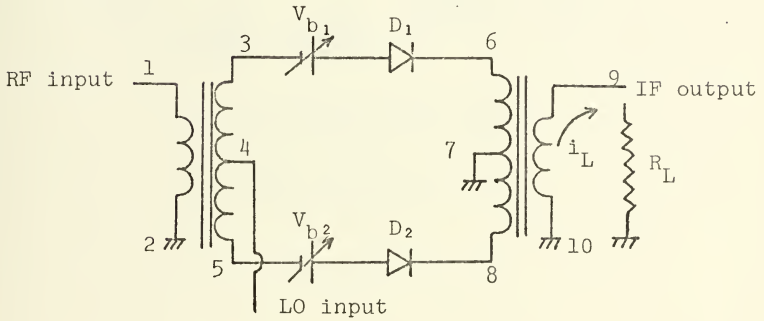

b. Single-Balanced Mixers.

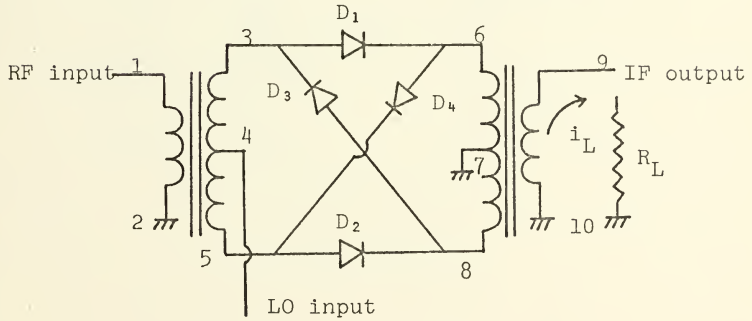

c. Double-Balanced Mixers.

FIGURE 1. Mixer Configurations.

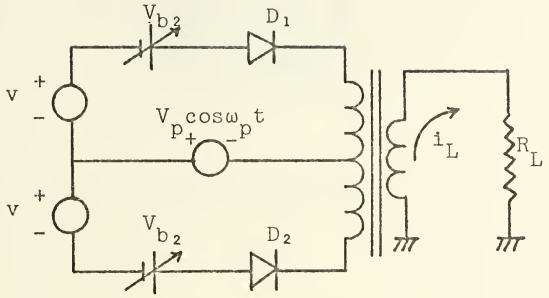

$$v = V_1 \cos\omega_1 t + V_2 \cos\omega_2 t$$

a. Single-Balanced Mixer

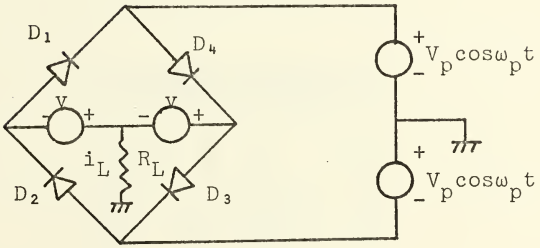

$$v = V_1 \cos\omega_1 t + V_2 \cos\omega_2 t$$

b. Double-Balanced Mixer.

FIGURE 2. Equivalent Circuits.

a. Single Diode Mixer.

b. Single-Balanced Mixer.

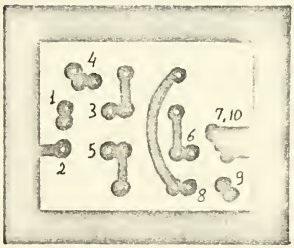

c. Double-Balanced Mixer.

FIGURE 3. Circuit-Boards.

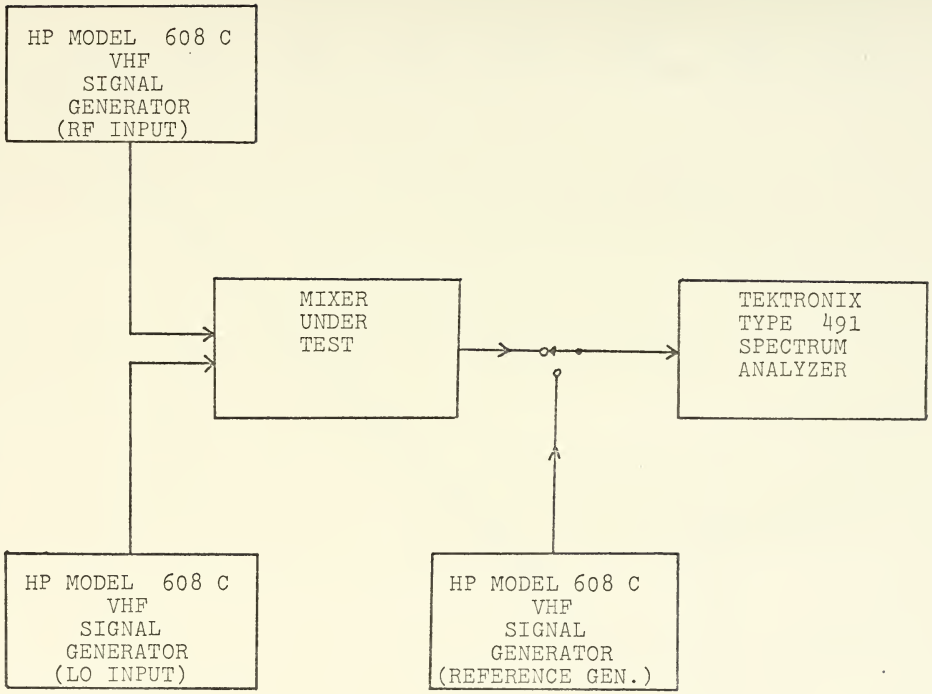

FIGURE 4. Experimental Setup.

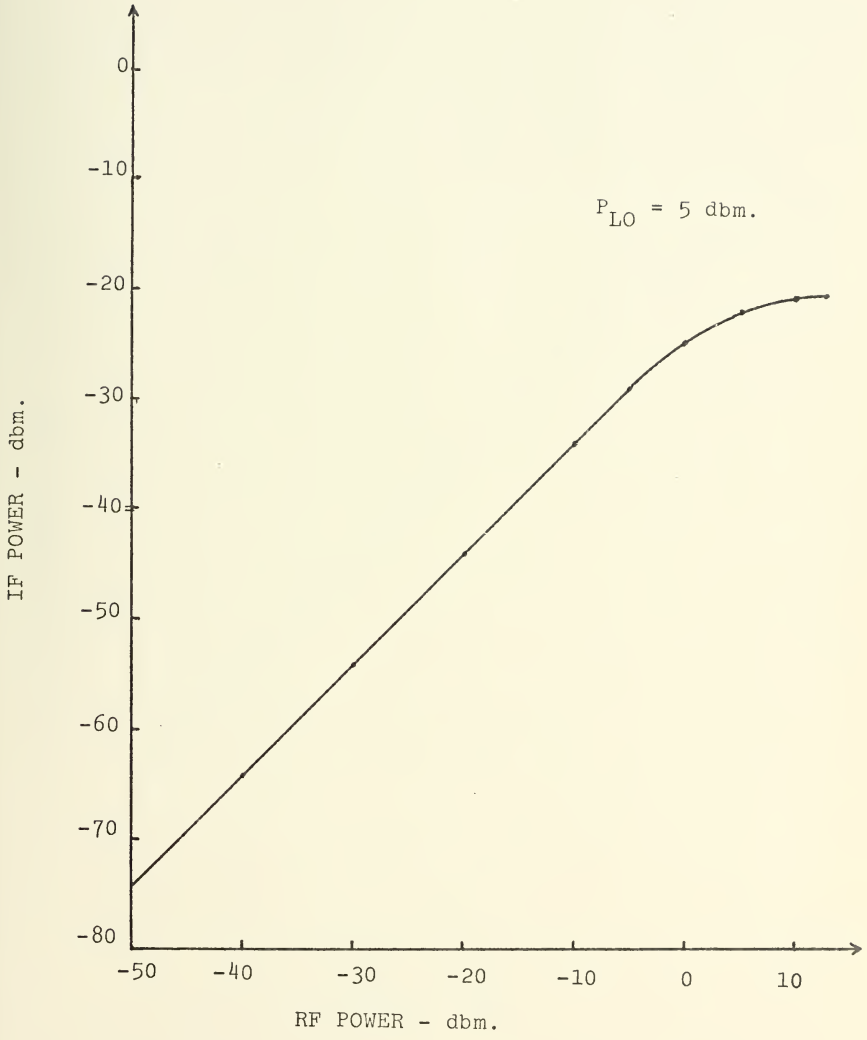

FIGURE 5. IF versus RF power for the single diode mixer.

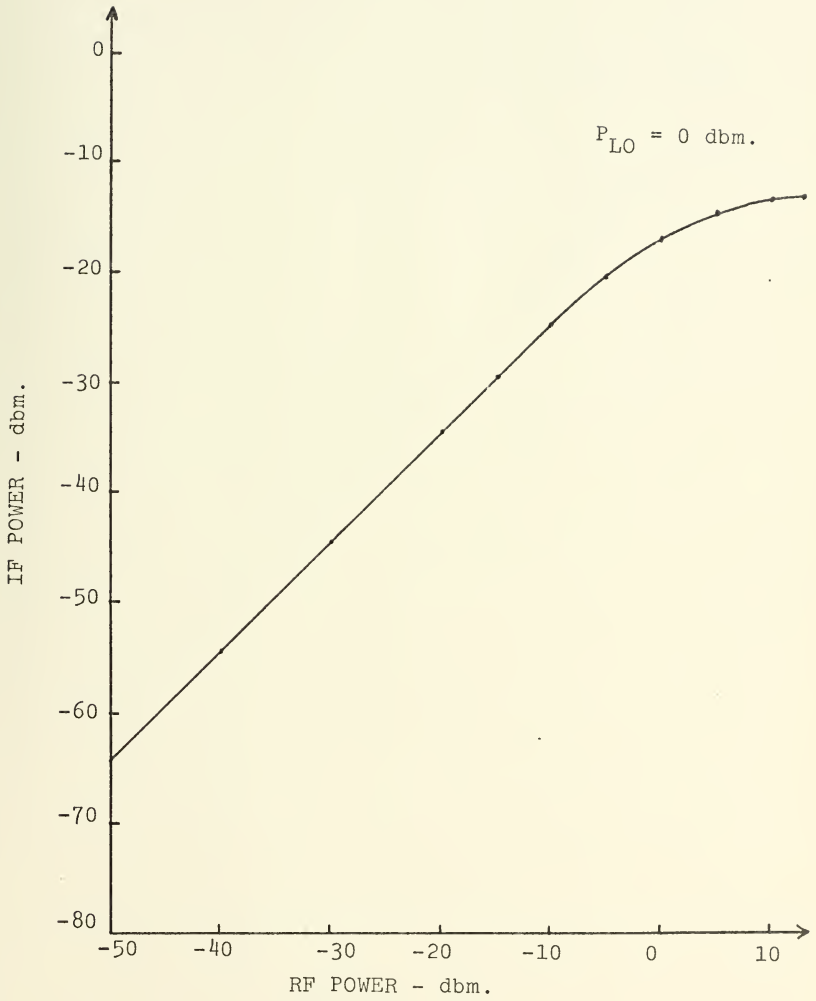

FIGURE 6. IF versus RF power for the single-balanced mixer.

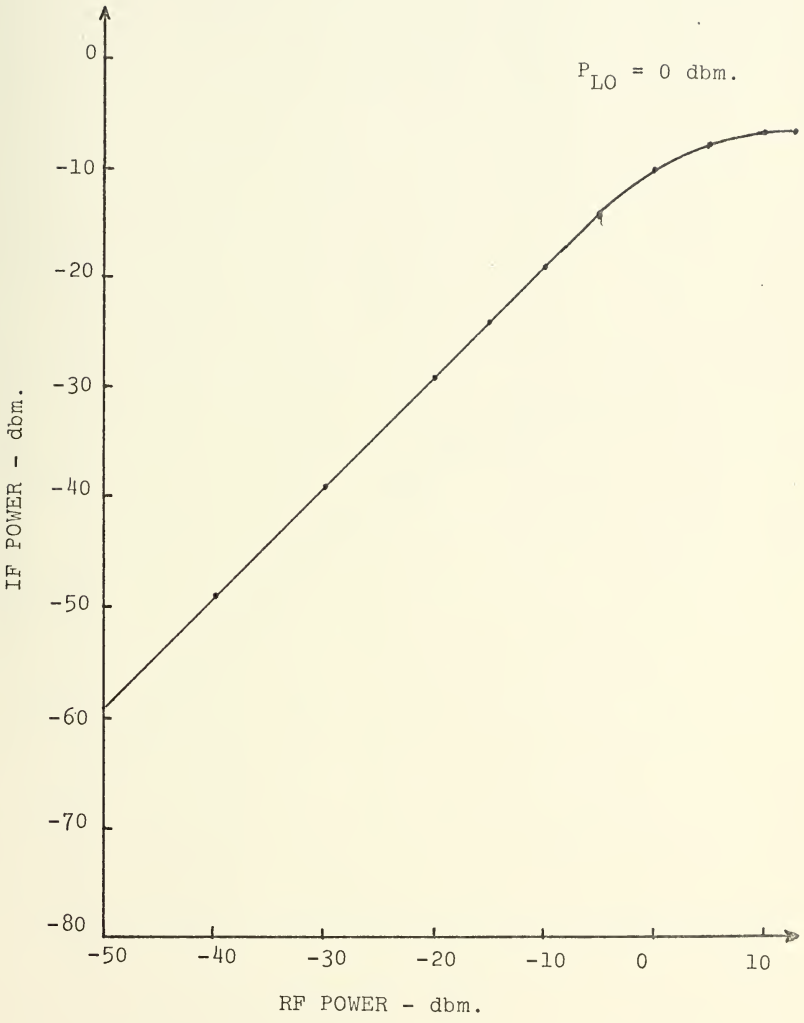

FIGURE 7. IF versus RF power for the double-balanced mixer.

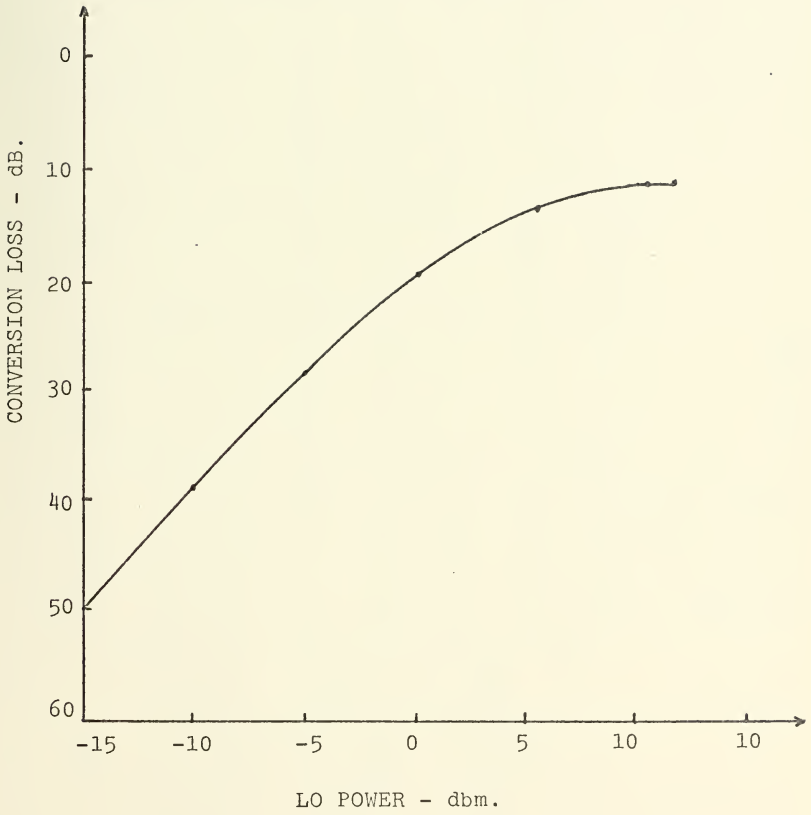

FIGURE 8. Conversion loss vs. LO power for the double-balanced mixer.

TYPE	THEORETICAL CONVERSION LOSS	MEASURED CONVERSION LOSS (AVG)	THEORETICAL RF ISOLATION	MEASURED RF ISOLATION (AVG.)	THEORETICAL LO ISOLATION	MEASURED LO ISOLATION (AVG.)
SINGLE DIODE MIXER	19.4 dB	25 dB	4 dB	20 dB	4 dB	20 dB
SINGLE-BALANCED MIXER	13.4 dB	14.5 dB	10 dB	26 dB	PERFECT	20 dB
DOUBLE-BALANCED MIXER	7.4 dB	9 dB	PERFECT	36 dB	PERFECT	42 dB

For theoretical value calculations,

$\alpha = 36.8$

$P_{RF} = -15$ dbm

$P_{LO} = 0$ dbm

$V_b = 0$ volt, are used.

TABLE I. Comparison of the mixers.

APPENDIX A: THEORETICAL ANALYSIS OF THE SINGLE DIODE MIXER

Current through the diode is:

$$i_1 = I_s(e^{\alpha V} - 1),$$

where,

$$v = V_b + V_b\cos\omega_1 t + V_2\cos\omega_2 t + V_p\cos\omega_p t$$

Then, the load current is

$$i_L = i_1 = I_s\left(e^{\alpha V_b}\, e^{\alpha V_1\cos\omega_1 t}\, e^{\alpha V_2\cos\omega_2 t}\, e^{\alpha V_p\cos\omega_p t} - 1\right).$$

Using the identity

$$e^{x\cos\theta} = I_o(x) + 2\sum_{r=1}^{\infty} I_r(x)\cos r\theta$$

$$i_L = I_s\Big[e^{\alpha V_b}(I_o(\alpha V_1) + 2\sum_{n=1}^{\infty} I_n(\alpha V_1)\cos n\omega_1 t)\cdot$$

$$(I_o(\alpha V_2) + 2\sum_{k=1}^{\infty} I_k(\alpha V_2)\cos k\omega_2 t)\cdot$$

$$(I_o(\alpha V_p) + 2\sum_{m=1}^{\infty} I_m(\alpha V_p)\cos m\omega_p t) - 1\Big].$$

$$i_L = I_s\Big\{ e^{\alpha V_b}\Big[I_o(\alpha V_1)I_o(\alpha V_2)I_o(\alpha V_p)$$

$$+2I_o(\alpha V_2)I_o(\alpha V_p)\sum_{n=1}^{\infty} I_n(\alpha V_1)\cos n\omega_1 t$$

$$+2I_o(\alpha V_1)I_o(\alpha V_p)\sum_{k=1}^{\infty} I_k(\alpha V_2)\cos k\omega_2 t$$

$$+2I_o(\alpha V_1)I_o(\alpha V_2)\sum_{m=1}^{\infty} I_m(\alpha V_p)\cos m\omega_p t$$

$$+4I_o(\alpha V_2)\sum_{n=1}^{\infty}\sum_{m=1}^{\infty} I_n(\alpha V_1)I_m(\alpha V_p)\cos n\omega_1 t\cdot\cos m\omega_p t$$

$$+4I_o(\alpha V_p)\sum_{n=1}^{\infty}\sum_{k=1}^{\infty} I_n(\alpha V_1)I_k(\alpha V_2)\cos n\omega_1 t\cdot\cos k\omega_2 t$$

$$+4I_o(\alpha V_1)\sum_{k=1}^{\infty}\sum_{m=1}^{\infty} I_k(\alpha V_2)I_m(\alpha V_p)\cos k\omega_2 t\cdot\cos m\omega_p t$$

$$+8\sum_{n=1}^{\infty}\sum_{k=1}^{\infty}\sum_{m=1}^{\infty} I_n(\alpha V_1)I_k(\alpha V_2)I_m(\alpha V_p)\cos n\omega_1 t\cdot \cos k\omega_2 t\cdot\cos m\omega_p t\Big]-1\Big\}.$$

Using $\cos a\cdot\cos b = \frac{1}{2}\cos(a\pm b)$,

$$i_L = I_s\Big\{ e^{\alpha V_b}\Big[I_o(\alpha V_1)I_o(\alpha V_2)I_o(\alpha V_p)$$

$$+2I_o(\alpha V_2)I_o(\alpha V_p)\sum_{n=1}^{\infty} I_n(\alpha V_1)\cos n\omega_1 t$$

$$+2I_o(\alpha V_1)I_o(\alpha V_p)\sum_{k=1}^{\infty} I_k(\alpha V_2)\cos k\omega_2 t$$

$$+2I_o(\alpha V_1)I_o(\alpha V_2)\sum_{m=1}^{\infty} I_m(\alpha V_p)\cos m\omega_p t$$

$$+2I_o(\alpha V_2)\sum_{n=1}^{\infty}\sum_{m=1}^{\infty} I_n(\alpha V_1)I_m(\alpha V_p)\cos(n\omega_1\pm m\omega_p)t$$

$$+2I_o(\alpha V_p)\sum_{n=1}^{\infty}\sum_{k=1}^{\infty} I_n(\alpha V_1)I_k(\alpha V_2)\cos(k\omega_2\pm n\omega_1)t$$

$$+2I_o(\alpha V_1)\sum_{k=1}^{\infty}\sum_{m=1}^{\infty} I_k(\alpha V_2)I_m(\alpha V_p)\cos(k\omega_2\pm m\omega_p)t$$

$$+2\sum_{n=1}^{\infty}\sum_{k=1}^{\infty}\sum_{m=1}^{\infty} I_n(\alpha V_1)I_k(\alpha V_2)I_m(\alpha V_p)\cdot$$

$$\cos(n\omega_1\pm k\omega_2\pm m\omega_p)t\Big]-1\Big\}.$$

APPENDIX B: THEORETICAL ANALYSIS OF THE BALANCED MIXER

$$i_1 = I_s(e^{\alpha v_1} - 1), \quad i_2 = I_s(e^{\alpha v_2} - 1)$$

where

$$v_1 = V_b + V_1\cos\omega_1 t + V_2\cos\omega_2 t + V_p\cos\omega_p t$$

and

$$v_2 = V_b - V_1\cos\omega_1 t - V_2\cos\omega_2 t + V_p\cos\omega_p t$$

Then,

$$i_L = i_1 - i_2$$

and

$$i_L = I_s\, e^{\alpha V_b}\left\{e^{\alpha V_1\cos\omega_1 t}\; e^{\alpha V_2\cos\omega_2 t}\; e^{\alpha V_p\cos\omega_p t} - e^{-\alpha V_1\cos\omega_1 t}\; e^{-\alpha V_2\cos\omega_2 t}\; e^{\alpha V_p\cos\omega_p t}\right\}.$$

Using the identities

$$e^{x\cos\theta} = I_o(x) + 2\sum_{r=1}^{\infty} I_r(x)\cos r\theta \qquad \text{(A-1)}$$

and

$$e^{-x\cos\theta} = I_o(x) + 2\sum_{r=1}^{\infty} I_r(x)\cos r(\theta+\pi) \qquad \text{(A-2)}$$

load current is found to be

$$i_L = I_s\, e^{\alpha V_b}\left(I_o(\alpha V_p) + 2\sum_{m=1}^{\infty} I_m(\alpha V_p)\cos m\omega_p t\right)$$

$$\left\{2I_o(\alpha V_1)\sum_{k=1}^{\infty} I_k(\alpha V_2)[\cos k\omega_2 t - \cos k(\omega_2 t+\pi)]\right.$$

$$\left. + 2I_o(\alpha V_2)\sum_{n=1}^{\infty} I_n(\alpha V_1)[\cos n\omega_1 t - \cos n(\omega_1 t+\pi)]\right.$$

$$+4 \sum_{n=1}^{\infty} \sum_{k=1}^{\infty} I_n(\alpha V_1) I_k(\alpha V_2) [\cos n\omega_1 t \cdot \cos k\omega_2 t - \cos n(\omega_1 t+\pi) \cos k(\omega_2 t+\pi)] \Bigg] .$$

Using

$$\cos q(x+\pi) = \cos qx \text{ for } q \text{ even and}$$

$$= -\cos qx \text{ for } q \text{ odd} \qquad \text{(A-3)}$$

$$i_L = I_s e^{\alpha V_b} \Bigg\{ I_o(\alpha V_p) \Bigg[4 I_o(\alpha V_1) \sum_{k=1,3,5,\ldots}^{\infty} I_k(\alpha V_2) \cdot \cos k\omega_2 t$$

$$+4 I_o(\alpha V_2) \sum_{n=1,3,5,\ldots}^{\infty} I_n(\alpha V_1) \cos n\omega_1 t$$

$$+8 \sum_{\substack{n=1,3,5,\ldots \\ n=2,4,6,\ldots}}^{\infty} \sum_{\substack{k=2,4,6,\ldots \\ k=1,3,5,\ldots}}^{\infty} I_n(\alpha V_1) I_k(\alpha V_2) \cos n\omega_1 t \cdot \cos k\omega_2 t \Bigg]$$

$$+8 I_o(\alpha V_1) \sum_{k=1,3,5,\ldots}^{\infty} \sum_{m=1}^{\infty} I_k(\alpha V_2) I_m(\alpha V_p) \cos k\omega_2 t \cdot \cos m\omega_p t$$

$$+8 I_o(\alpha V_2) \sum_{n=1,3,5,\ldots}^{\infty} \sum_{m=1}^{\infty} I_n(\alpha V_1) I_m(\alpha V_p) \cos n\omega_1 t \cdot \cos m\omega_p t$$

$$+16 \sum_{\substack{n=1,3,5,\ldots \\ n=2,4,6,\ldots}}^{\infty} \sum_{\substack{k=2,4,6,\ldots \\ k=1,3,5,\ldots}}^{\infty} \sum_{m=1}^{\infty} I_n(\alpha V_1) I_k(\alpha V_2) I_m(\alpha V_p) \cos n\omega_1 t \cdot \cos k\omega_2 t \cdot \cos m\omega_p t \Bigg\} .$$

Replacing $\cos a \cdot \cos b = \frac{1}{2}(a \pm b)$ (A-4)

$$i_L = I_s e^{\alpha V_b} \Bigg[4I_o(\alpha V_1)I_o(\alpha V_p) \sum_{k=1,3,5,\ldots}^{\infty} I_k(\alpha V_2)\cos k\omega_2 t$$

$$+4I_o(\alpha V_2)I_o(\alpha V_p) \sum_{n=1,3,5,\ldots}^{\infty} I_n(\alpha V_1) \cos n\omega_1 t$$

$$+4I_o(\alpha V_p) \sum_{\substack{n=1,3,5,\ldots \\ n=2,4,6,\ldots}}^{\infty} \sum_{\substack{k=2,4,6,\ldots \\ k=1,3,5,\ldots}}^{\infty} I_n(\alpha V_1)I_k(\alpha V_2) \cos(n\omega_1 \pm k\omega_2)t$$

$$+4I_o(\alpha V_1) \sum_{k=1,3,5,\ldots}^{\infty} \sum_{m=1}^{\infty} I_k(\alpha V_2)I_m(\alpha V_p)\cos(k\omega_2 \pm m\omega_p)t$$

$$+4I_o(\ V_2) \sum_{n=1,3,5,\ldots}^{\infty} \sum_{m=1}^{\infty} I_n(\alpha V_1)I_m(\alpha V_p)\cos(n\omega_1 \pm m\omega_p)t$$

$$+4 \sum_{\substack{n=1,3,5,\ldots \\ n=2,4,6,\ldots}}^{\infty} \sum_{\substack{k=2,4,6,\ldots \\ k=1,3,5,\ldots}}^{\infty} \sum_{m=1}^{\infty} I_n(\alpha V_1)I_k(\alpha V_2)I_m(\alpha V_p) \cos(n\omega_1 \pm k\omega_2 \pm m\omega_p)t \Bigg].$$

APPENDIX C: THEORETICAL ANALYSIS OF THE DOUBLE-BALANCED MIXER

$$i_1 = I_s(e^{\alpha v_1} - 1),$$

$$i_2 = I_s(e^{\alpha v_2} - 1),$$

$$i_3 = I_s(e^{\alpha v_3} - 1),$$

and

$$i_4 = I_s(e^{\alpha v_4} - 1).$$

Where

$$v_1 = V_1\cos\omega_1 t + V_2\cos\omega_2 t + V_p\cos\omega_p t,$$

$$v_2 = -V_1\cos\omega_1 t - V_2\cos\omega_2 t + V_p\cos\omega_p t,$$

$$v_3 = -V_1\cos\omega_1 t - V_2\cos\omega_2 t - V_p\cos\omega_p t,$$

and

$$v_4 = V_1\cos\omega_1 t + V_2\cos\omega_2 t - V_p\cos\omega_p t.$$

Load current

$$i_L = i_1 - i_2 + i_3 - i_4 \text{ and}$$

$$\frac{i_L}{I_s} = e^{\alpha V_1\cos\omega_1 t}\, e^{\alpha V_2\cos\omega_2 t}\, e^{\alpha V_p\cos\omega_p t}$$

$$-e^{-\alpha V_1\cos\omega_1 t}\, e^{-\alpha V_2\cos\omega_2 t}\, e^{\alpha V_p\cos\omega_p t}$$

$$+e^{-\alpha V_1\cos\omega_1 t}\, e^{-\alpha V_2\cos\omega_2 t}\, e^{-\alpha V_p\cos\omega_p t}$$

$$-e^{\alpha V_1\cos\omega_1 t}\, e^{\alpha V_2\cos\omega_2 t}\, e^{-\alpha V_p\cos\omega_p t}.$$

Using the identities (A-1) and (A-2) and arranging

$$\frac{i_L}{I_s} = \Big[I_o(\alpha V_1) I_o(\alpha V_2) + 2 I_o(\alpha V_2) \sum_{n=1}^{\infty} I_n(\alpha V_1) \cos n\omega_1 t$$

$$+ 2 I_o(\alpha V_1) \sum_{k=1}^{\infty} I_k(\alpha V_2) \cos k\omega_2 t$$

$$+ 4 \sum_{n=1}^{\infty} \sum_{k=1}^{\infty} I_n(\alpha V_1) I_k(\alpha V_2) \cos n\omega_1 t \cdot \cos k\omega_2 t \Big] \cdot$$

$$\{ 2 I_o(\alpha V_p) + 2 \sum_{m=1}^{\infty} I_n(\alpha V_p) [\cos m\omega_p t - \cos m(\omega_p t + \pi)] \}$$

$$- [I_o(\alpha V_1) I_o(\alpha V_2) + 2 I_o(\alpha V_2) \sum_{n=1}^{\infty} I_n(\alpha V_1) \cos n(\omega_1 t + \pi)$$

$$+ 2 I_o(\alpha V_1) \sum_{k=1}^{\infty} I_k(\alpha V_2) \cos k(\omega_2 t + \pi)$$

$$+ 4 \sum_{n=1}^{\infty} \sum_{k=1}^{\infty} I_n(\alpha V_1) I_k(\alpha V_2) \cos n(\omega_1 t + \pi) \cos k(\omega_2 t + \pi)] \cdot$$

$$\{ 2 I_o(\alpha V_p) + 2 \sum_{m=1}^{\infty} I_m(\alpha V_p) [\cos m\omega_p t - \cos m(\omega_p + \pi)] \}.$$

Replacing (A-3) and multiplying through,

$$\frac{i_L}{I_s} = 16 I_o(\alpha V_2) \sum_{n=1,3,5,\cdots}^{\infty} \sum_{m=1,3,5,\cdots}^{\infty} I_n(\alpha V_1) I_m(\alpha V_p)$$

$$\cos\omega_1 t \cdot \cos m\omega_1 t$$

$$+ 16 I_o(\alpha V_1) \sum_{k=1,3,5,\cdots}^{\infty} \sum_{m=1,3,5,\cdots}^{\infty} I_k(\alpha V_2) I_m(\alpha V_p)$$

$$\cos k\omega_2 t \cdot \cos m\omega_p t$$

$$+ 32 \sum_{\substack{n=1,3,5,\cdots \\ n=2,4,6,\cdots}}^{\infty} \sum_{\substack{k=2,4,6,\cdots \\ k=1,3,5,\cdots}}^{\infty} \sum_{m=1,3,5,\cdots}^{\infty} I_n(\alpha V_1) I_k(\alpha V_2)$$

$$I_m(\alpha V_p) \cos n\omega_1 t \cdot \cos k\omega_2 t \cdot \cos m\omega_p t.$$

Using (A-4)

$$\frac{i_L}{I_s} = 8I_o(\alpha V_2) \sum_{n=1,3,5,\cdots}^{\infty} \sum_{m=1,3,5,\cdots}^{\infty} I_n(\alpha V_1) I_m(\alpha V_p) \cos(n\omega_1 \pm m\omega_p)t$$

$$+8I_o(\alpha V_1) \sum_{k=1,3,5,\cdots}^{\infty} \sum_{m=1,3,5,\cdots}^{\infty} I_k(\alpha V_2) I_m(\alpha V_p) \cos(k\omega_2 \pm m\omega_p)t$$

$$+8 \sum_{\substack{n=1,3,5,\cdots \\ n=2,4,6,\cdots}}^{\infty} \sum_{\substack{k=2,4,6,\cdots \\ k=1,3,5,\cdots}}^{\infty} \sum_{m=1,3,5,\cdots}^{\infty} I_n(\alpha V_1) I_k(\alpha V_2) I_m(\alpha V_p) \cos(n\omega_1 \pm k\omega_2 \pm m\omega_p)t.$$

LIST OF REFERENCES

1. Belevitch, V., "Linear Theory of Bridge and Ring Modulator Circuits", Electrical Communication, Vol. 25, No. 1, p. 62, March 1948

2. Airborne Instruments Laboratory Technical Report No. RADC-TR-66-610, Preferred-Circuit Techniques for Crystal Diode Mixers, by J. Coniglione and G. Kanischak, p. 2-1, November 1966.

3. Crane, M. and Sorensen, H. O., "Using the Hot-Carrier Diode as a Detector", Hewlett-Packard Journal, Vol. 17, No. 4, p. 3-5, December 1965.

4. Ernst, R. L., Terrione, R., Pan, W. Y., and Morris, M. M., "Designing Microwave Mixers for Increased Dynamic Range", IEEE Transcripts on Electromagnetic Compatibility, Vol. EMC-11, No. 4, p. 130-138, November 1969.

5. Fischer, R., "An Engineers Ham-Band Receiver", QST, Vol. LIV, No. 3, p. 11, March 1970.

6. Gretsch, W. R., "The Spectrum of Intermodulation Generated in a Semiconductor Diode Function", Proceedings of IEEE, Vol. 54, No. 11, p. 1528, November 1966.

7. Herishen, J. T., "Diode Mixer Coefficients for Spurious Response Prediction", IEEE Transactions on Electromagnetic Compatibility, Vol. EMC-10, No. 4, p. 355, December 1968.

8. Airborne Instruments Laboratory Technical Report No. RADC-TR-67-216, Preferred-Circuit Techniques for Receiver Applications, by G. Kanischak, S. Becker, and D. Kornfeld, p. 5.1, June 1967.

9. Orloff, L. M., "Intermodulation Analysis of Crystal Mixers", Proceedings of IEEE, Vol. 52, No. 2, p. 173, February 1964.

10. Ress, W., "Broadband Double-Balanced Modulator", Ham Radio, Vol. 3, No. 3, p. 8, March 1970.

11. Tucker, D. G., "Intermodulation Distortion in Rectifier Modulators", Wireless Engineer, Vol. 31, No. 6, p. 145, June 1954.

INITIAL DISTRIBUTION LIST

		No. Copies
1.	Defense Documentation Center Cameron Station Alexandria, Virginia 22314	2
2.	Library, Code 0212 Naval Postgraduate School Monterey, California 93940	2
3.	Professor R. W. Adler, Code 52AB Department of Electrical Engineering Naval Postgraduate School Monterey, California 93940	1
4.	Lt. (jg) Ersin Güler, Turkish Navy Kiztasi, Haci Salih Efendi Sok. 39/1 Fatih, Istanbul Turkey	5
5.	Istanbul Teknik Üniversitesi Elektrik Fakültesi Taskisla, Istanbul Turkey	1
6.	Orta-Dogu Teknik Üniversitesi Elektrik Fakültesi Ankara, Turkey	1
7.	Karadeniz Teknik Üniversitesi Elektrik Fakültesi Trabzon, Turkey	1
8.	Robert College School of Engineering Bebek, Istanbul Turkey	1
9.	Deniz Kuvvetleri Komutanliği Personel Eğitim Sb. Müdürlügü Ankara, Turkey	1
10.	Deniz Harb Okulu Komutanliği Heybeliada, Istanbul Turkey	1

11. Deniz Makine Sinif Okullari Komutanligi 1
Derince, Kocaeli
Turkey

UNCLASSIFIED
Security Classification

DOCUMENT CONTROL DATA - R & D

(Security classification of title, body of abstract and indexing annotation must be entered when the overall report is classified)

1. ORIGINATING ACTIVITY (Corporate author)

Naval Postgraduate School
Monterey, California 93940

2a. REPORT SECURITY CLASSIFICATION

UNCLASSIFIED

2b. GROUP

3. REPORT TITLE

A Study of Broadband Hot-Carrier Diode Mixers

4. DESCRIPTIVE NOTES (Type of report and, inclusive dates)

Master's Thesis, December 1970

5. AUTHOR(S) (First name, middle initial, last name)

Ersin Güler

6. REPORT DATE	7a. TOTAL NO. OF PAGES	7b. NO. OF REFS
December 1970	49	11

8a. CONTRACT OR GRANT NO	9a. ORIGINATOR'S REPORT NUMBER(S)
b. PROJECT NO.	
c.	9b. OTHER REPORT NO(S) (Any other numbers that may be assigned this report)
d.	

10. DISTRIBUTION STATEMENT

This document has been approved for public release and sale; its distribution is unlimited.

11. SUPPLEMENTARY NOTES	12. SPONSORING MILITARY ACTIVITY
	Naval Postgraduate School Monterey, California 93940

13. ABSTRACT

A theory is derived for single diode, single-balanced, and double-balanced mixers. An interfering signal is assumed to be present in order to analyze intermodulation and cross-modulation distortions.

Measurements are made in the 50 - 200 MHz range and close agreement with the theory is found for conversion loss. Disagreement in RF and LO isolations is attributed to stray capacitances. It is also shown that circuit-board and transformer design greatly affects performance of a mixer.

A comparison of the single diode, single-balanced, and double-balanced mixers is given and it is indicated that the double-balanced mixer is superior.

14 KEY WORDS	LINK A		LINK B		LINK C	
	ROLE	WT	ROLE	WT	ROLE	WT
Mixing Circuits						
Crystal Mixers